



Measurement of $t\bar{t}$ Production Cross Section in the Lepton + Tau + b-jet(s) + Missing Transverse Energy Channel Using 1 fb^{-1} of Run II Data

The DØ Collaboration
URL <http://www-d0.fnal.gov>

We describe a measurement of the production cross section of top quark-antitop quark pairs in the lepton+tau channel in approximately 1 fb^{-1} of data, collected using the DØ detector at the Fermilab Tevatron $p\bar{p}$ collider during April 2002 through February 2006. We select events with one isolated high p_T electron or muon, one isolated hadronic tau candidate, missing transverse energy, and two or more high p_T jets. Signal to background is improved by applying a neural network b -tagging algorithm. We find 29 candidate events in the $\mu + \tau$ channel, and 18 candidate events in the $e + \tau$ channel. We measure both the top pair production cross section (assuming standard model decay ratios) and the cross section times branching ratio (assuming standard model cross section for top events other than those with a real lepton and real tau in the final state) as:

$$\sigma(t\bar{t}) = 8.3_{-1.8}^{+2.0} (\text{stat})_{-1.2}^{+1.4} (\text{syst}) \pm 0.5 (\text{lumi}) \text{ pb},$$

$$\sigma(t\bar{t}) \times BR(t\bar{t} \rightarrow \ell + \tau + 2\nu + 2b) = 0.19_{-0.08}^{+0.08} (\text{stat})_{-0.07}^{+0.07} (\text{syst}) \pm 0.01 (\text{lumi}) \text{ pb}.$$

Preliminary Results for Summer 2007 Conferences

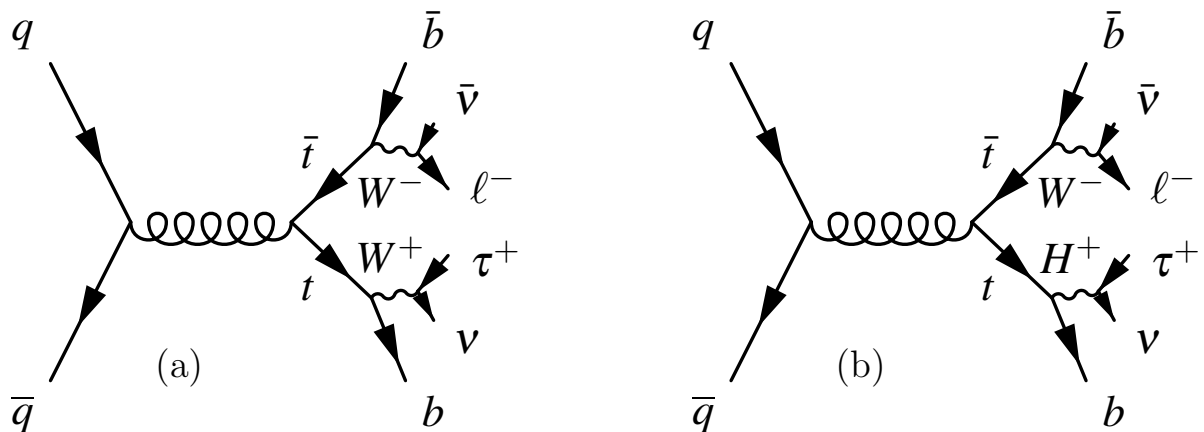


FIG. 1: Feynman diagrams for (a) standard model top pair production with decay to $\ell + \tau + 2\nu + 2b$ and (b) with top decay to a charged Higgs boson + b quark.

I. INTRODUCTION

The cross section for pair production of top quarks has been measured in numerous channels at the Tevatron including dileptons [1, 2], lepton + jets [3, 4], and all jets [5, 6]. Final states involving taus are the last remaining standard model decay modes to be studied. Recently DØ performed a measurement in the τ + jets channel [7]. This note describes a measurement using the $\ell + \tau + 2b + 2\nu$ final states where $\ell = e$ or μ and the τ decays hadronically (τ_h) (see Fig. 1(a)). We study events with one reconstructed lepton, one τ candidate, two or more jets with at least one tagged as a heavy flavor jet and missing transverse energy (\cancel{E}_T).

There are several reasons to study the $\ell + \tau + b$ -jets + \cancel{E}_T channel. The first is to measure the top pair production cross section with additional data. This analysis provides one of the larger dilepton samples of top pair events. The second is to probe for new physics by measuring the cross section times branching ratio and comparing it to other decay modes. For example, if there exists a charged Higgs boson with $m_{H^+} < m_t - m_b$, an enhancement in the tau channel might be observed through $t \rightarrow H^+ b \rightarrow \tau \nu b$ (see Fig. 1(b)). This would lead to an excess of events in this channel given $\text{BR}(H \rightarrow \tau \nu) > \text{BR}(W \rightarrow \tau \nu)$.

The final event sample is dominated by top quark events which include decays to $\ell + \tau + 2\nu + 2b$, other dilepton states and ℓ +jet states. In this note, we present a two stage analysis:

1. First, we measure the top production cross-section using all available top events assuming standard model branching ratios. This result can be combined with other measurements by accounting for any overlap between samples.
2. Second, we measure the cross-section \times branching ratio for the specific final states $t\bar{t} \rightarrow \mu/e + \tau_h + 2\nu + 2b$.

The $\mu\tau$ and $e\tau$ samples are studied independently and combined in the final stage of the analysis. The integrated luminosities for the $\mu\tau$ and $e\tau$ analyses are $994 \pm 61 \text{ pb}^{-1}$ and $1036 \pm 63 \text{ pb}^{-1}$, respectively [8].

II. EVENT RECONSTRUCTION

The DØ detector consists of a central tracking system, calorimeter, and outer muon system. The central tracking system surrounds the interaction region with a silicon microstrip detector (SMT) and a fiber tracker (CFT) within a 2T solenoidal magnet. A preshower detector lies between the solenoidal magnet and the calorimeter for improved identification of electrons, photons, and taus. The calorimeter is composed of liquid argon calorimeter and intercalorimeter detector (ICD). The calorimeter is divided into a central region ($|\eta| < 1.1$) and a forward region ($1.4 < |\eta| < 2.5$). The ICD covers the intermediate region. The outer muon system contains 3 layers of scintillators and drift tubes with a toroid magnet between the first two layers. Additional details of the detector are available [9].

Electrons are reconstructed in the electromagnetic (EM) and hadronic layers (HAD) of the calorimeter by clustering energy in cells within a cone of $\Delta R = \sqrt{\Delta\phi^2 + \Delta\eta^2} < 0.4$. They are required to be in the central region of the

calorimeter ($|\eta| < 1.1$) and more than 90% of the energy must lie in the EM layers. A central track must be spatially matched to the cluster, and it must be isolated from significant energy in the hadronic calorimeter. A likelihood discriminant identifies electrons using information on the shower shape and central track [10].

Muons must be reconstructed in all three layers of the muon system. We consider muons which are reconstructed with $|\eta| < 2.0$. They must be matched to a track in the central tracking system with $\chi^2/n.d.o.f < 4$. Cosmic ray muons are rejected by requiring the muons to pass timing cuts. The distance of closest approach of the central track to the event's primary vertex on the $x - y$ plane must be $< 0.02(0.2)$ cm for tracks with(without) hits in the SMT. Two criteria were used for muon isolation: (1) the sum of the energy deposited in the calorimeter within a hollow cone of $0.1 < \Delta R < 0.4$ must be less than 15% of the muon energy, and (2) the sum of the p_T of tracks surrounding the muon within $\Delta R < 0.5$ must be less than 15% of the muon p_T [10].

Jets are reconstructed from energy in the calorimeter using a fixed cone algorithm with cone size $\Delta R < 0.5$ [11]. They must be reconstructed within $|\eta| < 2.5$. A minimum transverse momentum of 6 GeV is required at reconstruction. We include requirements on Level 1 calorimeter trigger match, calorimeter electromagnetic fraction, and calorimeter coarse hadronic fraction. The missing transverse energy (E_T^{miss}) is calculated by performing a vectorial sum of the transverse energies deposited in the calorimeter. This sum is then corrected with the momenta of well-reconstructed muons, and corrected energies of well-reconstructed electrons and jets in the events.

Taus are reconstructed from energy in the calorimeter and one or more tracks. The tau cone reconstruction algorithm uses a cone size of $\Delta R < 0.5$. An inner cone of size $\Delta R < 0.3$ is used to calculate tau isolation variables. We required that they are inside the central region of the calorimeter ($|\eta| < 1.0$). An electromagnetic sub cluster may also be associated with the tau candidate. Tracks (ordered in decreasing p_T) within a cone of $\Delta R < 0.5$ may be matched to the tau candidate as long as their z -position is within 2 cm of the first track at closest approach, the mass calculated using the tracks is less than the tau mass, and no more than three tracks are already matched. The reconstructed tau candidates are classified into three categories:

1. **Type 1:** One track without any associated electromagnetic sub clusters. This type of tau candidate is expected to come from the decay

$$\tau^- \rightarrow \pi^- + \nu_\tau.$$

2. **Type 2:** One track with associated electromagnetic sub cluster. This type of tau candidate is expected to come from the decay

$$\tau^- \rightarrow \pi^- + n\pi^0 + \nu_\tau,$$

where there are $n \geq 1$ neutral pions.

3. **Type 3:** Two or three tracks. This type of tau candidate is expected to come from the decay

$$\tau^- \rightarrow \pi^- \pi^+ \pi^- + \nu_\tau + n\pi^0,$$

where there can be $n \geq 0$ neutral pions.

A neural network (NN_τ) has been trained to separate real taus from jets which fake taus. The NN_τ uses variables which emphasize the difference of taus from jets: low track multiplicity, narrow calorimeter clusters, isolation in the central tracking system and the calorimeter, and correlation between the track(s) and calorimeter cluster(s). The variables are derived from tau tracks, hadronic and electromagnetic calorimeter cluster energies, shower shape, and the detector geometry. Additional description of some of the variables can be found in Ref. [12]. Figure 2 shows the distributions of NN_τ for two ranges of NN_τ value. We require taus to have $NN_\tau > 0.8$. Using $W(\rightarrow e\nu)$ +jets events, we determine a data/MC correction factor on the rate for fake taus from jets of 1.07 ± 0.12 .

A second neural network (NN_{elec}) is used to separate tau type 2 and electrons. For NN_{elec} , the neural net uses a subset of the input variables of NN_τ , and variables based on the electromagnetic cluster and correlation between electromagnetic cluster and the leading tau track. Figure 3 illustrates the rejection of fake taus from the NN_τ and NN_{elec} variables. The $e\tau$ analysis requires taus to pass $NN_{elec} > 0.8$. In addition the $e\tau$ analysis removes tau candidates with track ϕ less than 0.02 radian from the nearest calorimeter module wall, which are likely mis-measured electrons.

The presence of one or more jets coming from a b -quark is a powerful discriminator between signal top quark events and background events. In this analysis we use a neural network (NN_b) algorithm to identify if a jet originated from a b -quark. We require data events to have at least one jet with $NN_b > 0.65$ which results in an average efficiency of 54% for b -jets and an average fake rate of 1%. In Monte Carlo (MC) events, we assign a probability to each jet in the event to have originated from a b -quark. This probability is measured from data and is often referred to as the "tag rate function". To increase the statistical power in Monte Carlo events, we consider all possible permutations of applying the tagging algorithm. This follows a similar procedure to the single top analysis [13].

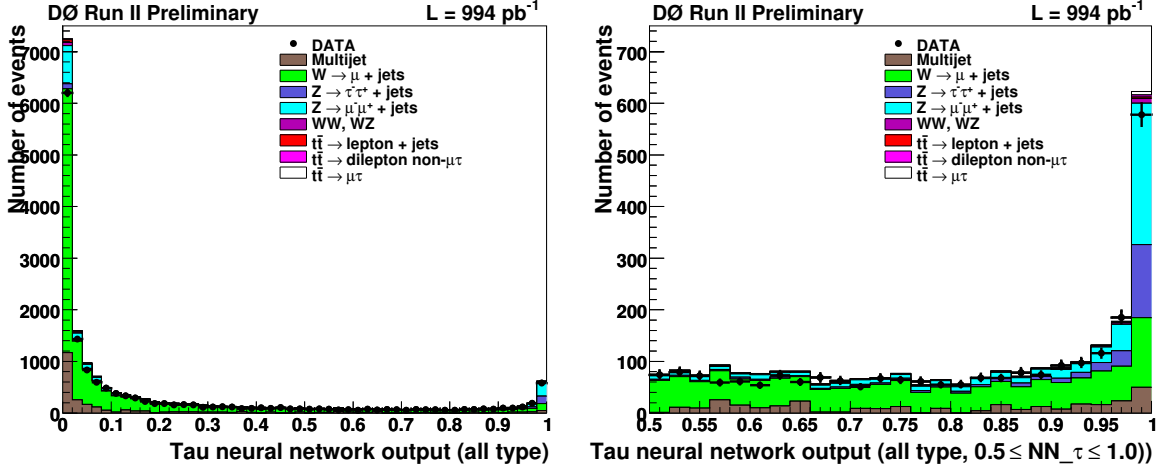


FIG. 2: Distributions of tau neural network output (NN_τ) in the $\mu\tau$ channel. Shown are the distributions in the $[0.0, 1.0]$ interval (left figure), and in the zoomed $[0.5, 1.0]$ interval (right figure). These are made prior to NN_τ , \cancel{E}_T , jet-tau matching, and b -tagging criteria.

III. SIGNAL AND BACKGROUND MODELS

Signal and most backgrounds are generated using ALPGEN v2.05 [14] interfaced with PYTHIA v6.323 [15]. Standard model backgrounds considered include W +jets, Z/γ^* +jets (in the ee , $\mu\mu$, and $\tau\tau$ decay modes), dibosons, estimated using MC, and multijet events, estimated from data. $t\bar{t}$ acts as both a background and signal under different parts of the analyses. We have generated both $t\bar{t} \rightarrow$ dileptons and $t\bar{t} \rightarrow$ lepton + jets with a top mass of 175 GeV. The W MC is normalized to data by fitting the transverse mass distribution after only requiring an isolated muon or electron, one or more jets, and missing transverse energy. The template for multijet events at this selection stage is obtained from events which have a non-isolated muon or electron, one or more jets, and missing transverse energy. We subtract the estimated contributions of $Z\gamma$ +jets, $t\bar{t}$, and dibosons events before performing the fit. The Z/γ^* MC is normalized to the next-to-leading order (NLO) cross section [16]. In both cases an additional factor (1.17 for W and 1.1 for Z/γ^*) scales the heavy quark component to match the heavy/light ratio in NLO calculations.

The multijet background is modeled from data using events with the lepton and τ having the same-sign (SS) charge. We subtract from this sample contributions from MC W and $t\bar{t}$ same-sign events to predict the number of multijet events in the final samples. $t\bar{t}$ contributions to the same-sign sample result from either a random jet being reconstructed as a tau or from charge mis-id of a real tau. Contributions of Z/γ^* and diboson to the SS sample are small.

$$N_{multijet}^{OS} = N_{multijet}^{SS} = N_{DATA}^{SS} - N_{W+jets}^{SS} - N_{t\bar{t}}^{SS}. \quad (1)$$

IV. SELECTION CRITERIA

We use data collected during April, 2002 to February, 2006. The $\mu\tau$ analysis uses a trigger that requires a muon and a jet with $p_T > 20, 25, 35$ GeV depending on the running period, while the $e\tau$ analysis uses a trigger with an electron and two jets (one of which has $p_T > 20, 25, 30$ GeV). Standard criteria are applied for data quality and primary vertex requirements. Events are required to have either an isolated muon ($p_T > 20$ GeV) or an isolated electron ($p_T > 15$ GeV) as described in Sec. II. Events containing either a second lepton of the same type or an isolated lepton of the opposite type (μ/e) are rejected to reduce $Z \rightarrow \mu\mu/ee$ background and ensure orthogonality with existing dilepton analyses. At least one jet with $p_T > 30$ GeV is required. Any other jet must have $p_T > 20$ GeV. Because of the presence of several neutrinos, we require $15 < \cancel{E}_T < 200$ GeV. Each event must have at least one tau candidate. If more than one tau is found, the one with the highest NN_τ is used and other tau candidates are ignored. The list of

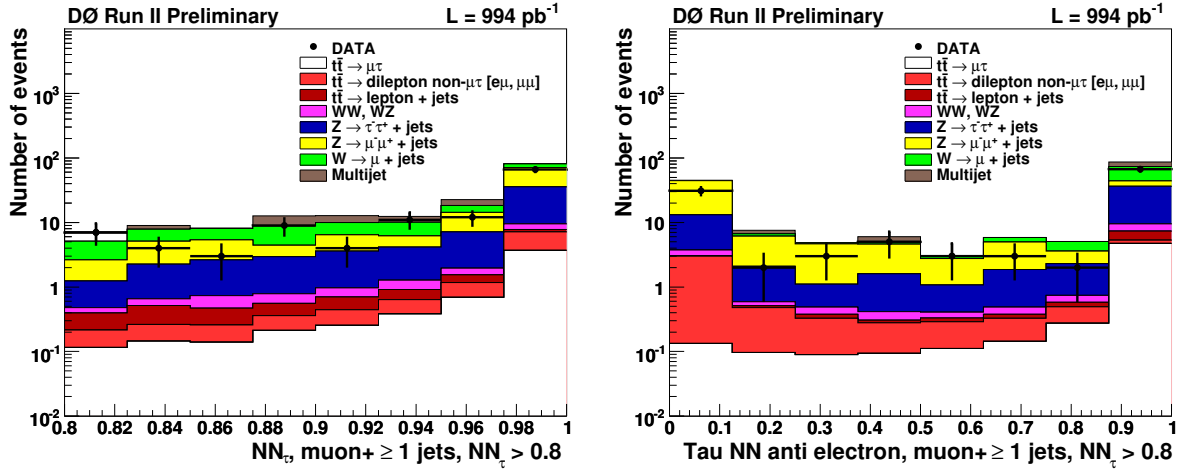


FIG. 3: Distributions of output from tau neural network to reject jet (NN_τ , left figure) and tau neural network anti electron (NN_{elec} , right figure) in the $\mu\tau$ channel. In this sample, the major components which contain fake taus from electrons are $t\bar{t} \rightarrow$ other dilepton and $Z \rightarrow \tau\tau \rightarrow \tau e T_{had}$. Left figure shows that NN_τ can't distinguish electrons which fake taus from real taus, while the right figure shows that NN_{elec} can. These are made with muon, tau, \cancel{E}_T , and jet requirements but no b -tagging.

TABLE I: Data and predicted numbers of events before and after b -tagging is applied. Standard model cross section and branching ratios are assumed for $t\bar{t}$ production. Uncertainties are statistical only.

	before b -tagging		after b -tagging	
	$\mu\tau$	$e\tau$	$\mu\tau$	$e\tau$
W	38.0 ± 1.7	34.1 ± 3.5	2.31 ± 0.22	2.13 ± 0.27
$Z/\gamma^* \rightarrow ee$ or $\mu\mu$	20.7 ± 1.1	5.8 ± 0.6	1.09 ± 0.11	0.38 ± 0.05
$Z/\gamma^* \rightarrow \tau\tau$	19.6 ± 1.2	7.5 ± 0.6	1.02 ± 0.10	0.54 ± 0.06
Diboson	2.8 ± 0.1	5.1 ± 0.6	0.21 ± 0.01	0.34 ± 0.07
Multijet	10.6 ± 6.3	12.7 ± 6.6	4.52 ± 3.01	-1.27 ± 1.77
$t\bar{t} \rightarrow \ell + \tau + 2b + 2\nu$	7.8 ± 0.1	6.67 ± 0.1	5.64 ± 0.04	4.70 ± 0.05
$t\bar{t} \rightarrow$ other dileptons	4.3 ± 0.1	0.73 ± 0.1	3.14 ± 0.03	0.47 ± 0.07
$t\bar{t} \rightarrow \ell +$ jets	12.7 ± 0.1	12.41 ± 0.2	8.40 ± 0.11	7.88 ± 0.12
Total Expected	116.6 ± 6.8	85.0 ± 7.7	26.33 ± 3.02	15.17 ± 1.97
Data	104	69	29	18

jets is redone, removing any jet that falls within $\Delta R < 0.5$ of this tau candidate. At this point, at least two jets are required. All of the above criteria are applied to both analyses.

For the $\mu\tau$ analysis, events with a second non-isolated muon are rejected if the invariant mass of the two muons lies in the range $70 < m_{\mu\mu} < 100$ GeV. In the $e\tau$ analysis the electron-tau fake rejection is applied and we reject events where the electron and \cancel{E}_T line up in ϕ by requiring $\cos(\Delta\phi(e, \cancel{E}_T)) < 0.9$. The remaining events are referred to as the pre-tag sample. The final selection criteria is that at least one of the jets be tagged as coming from a b -quark (tagged sample). This dramatically improves the signal-to-background and this sample is used for the cross section measurements. Table I lists the observed and expected numbers of events at the pre-tag and tagged stages. Figures 4 and 5 show distributions from the $\mu\tau$ and $e\tau$ samples (combined), before and after b -tagging.

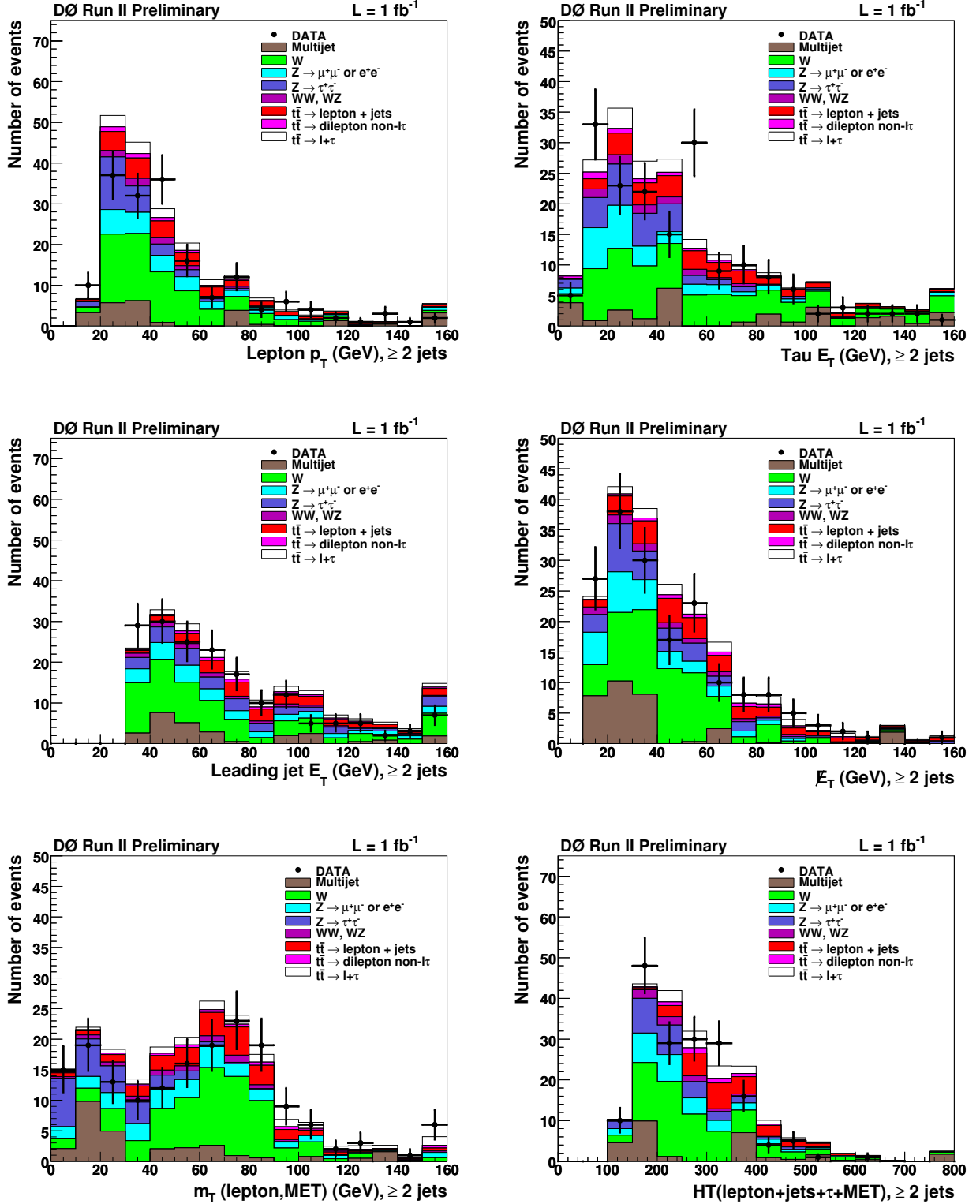


FIG. 4: Distributions comparing $\mu\tau + e\tau$ data to expectations before b -tagging is applied. This is done assuming a standard model cross section for top pair production. Overflows are placed in the rightmost bin. “lepton” = μ or e . The distributions are: lepton p_T (top left); τp_T (top right); leading jet p_T (middle left); missing transverse energy (E_T) (middle right); lepton- E_T transverse mass, $m_T = \sqrt{(E_T + p_T^l)^2 - (E_x + p_x^l)^2 - (E_y + p_y^l)^2}$ (bottom left); H_T is the magnitude of the vector sum of the lepton’s, the tau’s, all jets’s, and E_T ’s transverse momentum (bottom right).

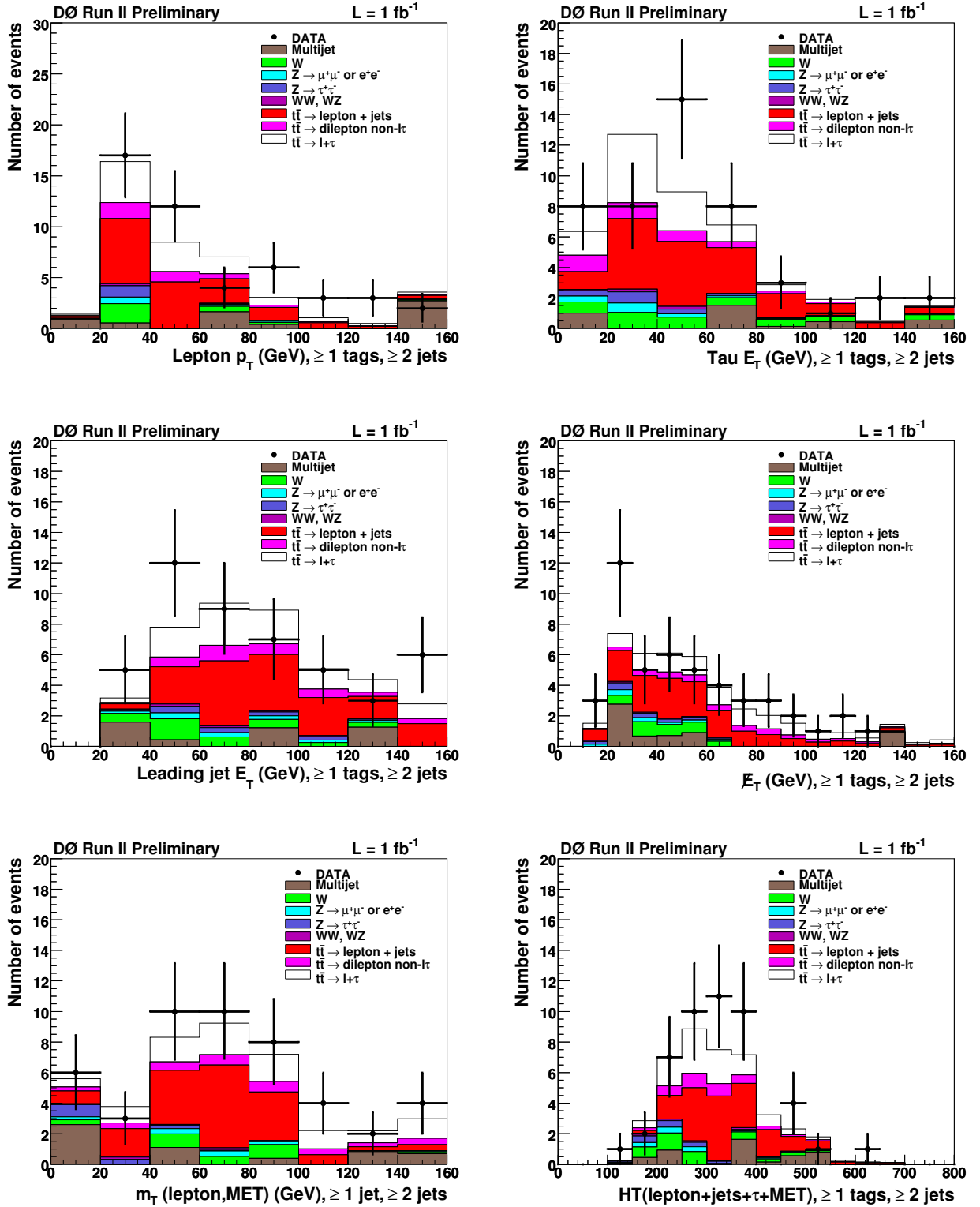


FIG. 5: Distributions comparing $\mu\tau + e\tau$ data to expectations after b -tagging is applied. This is done assuming a standard model cross section for top pair production. Overflows are placed in the rightmost bin. “lepton” = μ or e . The distributions are: lepton p_T (top left); τp_T (top right); leading jet p_T (middle left); missing transverse energy (E_T) (middle right); lepton- E_T transverse mass, $m_T = \sqrt{(E_T + p_T^l)^2 - (E_x + p_x^l)^2 - (E_y + p_y^l)^2}$ (bottom left); H_T is the magnitude of the vector sum of the lepton’s, the tau’s, all jets’, and E_T ’s transverse momentum (bottom right).

TABLE II: Acceptances (in unit of %) of the lepton+tau+b-jet(s)+ \cancel{E}_T selection for $t\bar{t} \rightarrow$ dilepton, $t\bar{t} \rightarrow$ lepton+jets, $t\bar{t} \rightarrow$ inclusive and $t\bar{t} \rightarrow \ell + \tau + 2b + 2\nu$ samples. The top section shows the acceptance for opposite-sign events taking into account the SM BR, the middle section is for same-sign events using the SM BR, and the bottom section is for opposite-sign $\ell + \tau + 2b + 2\nu$ signal without BR. Uncertainties are statistical only.

Process	$\mu\tau$ acceptance	$e\tau$ acceptance
Opposite-signed $t\bar{t}$		
$t\bar{t} \rightarrow$ dilepton	0.1304 ± 0.0015	0.0761 ± 0.0012
$t\bar{t} \rightarrow$ lepton+jets	0.1247 ± 0.0027	0.1117 ± 0.0025
$t\bar{t} \rightarrow$ inclusive	0.2551 ± 0.0031	0.1878 ± 0.0028
Same-signed $t\bar{t}$		
$t\bar{t} \rightarrow$ dilepton	0.0025 ± 0.0002	0.0026 ± 0.0002
$t\bar{t} \rightarrow$ lepton+jets	0.0459 ± 0.0020	0.0421 ± 0.0015
$t\bar{t} \rightarrow$ inclusive	0.0484 ± 0.0020	0.0447 ± 0.0015
$t\bar{t} \rightarrow \ell + \tau + 2b + 2\nu$ (no BR)	4.59 ± 0.03	3.85 ± 0.06

V. CROSS SECTION EXTRACTION

First, we measure the top pair production cross section assuming standard model branching ratios. Here we use all top pair events which reconstruct in our final state as signal, including those with fake taus from jets or leptons. Backgrounds include W , $Z/\gamma^* \rightarrow \mu\mu$ or ee , $Z/\gamma^* \rightarrow \tau\tau$, dibosons and multijet events (Table I). The number of data events in the opposite-sign (OS) sample is given by

$$N_{DATA}^{OS} = N_{t\bar{t}}^{OS} + N_W^{OS} + N_Z^{OS} + N_{Diboson}^{OS} + N_{Multijet}^{OS}, \quad (2)$$

where $N_{t\bar{t}}^{OS}$ is the signal sample. Because we subtract same-sign $t\bar{t}$ events from same-sign data in calculating the multijet background (Eq. 1), top production contributes twice to the expected numbers of events. Therefore we measure the cross-section by

$$\sigma_{t\bar{t}} = \frac{N_{DATA}^{OS} - N_{DATA}^{SS} - (N_W^{OS} - N_W^{SS}) - N_Z^{OS} - N_{Diboson}^{OS}}{(\epsilon_{t\bar{t}}^{OS} - \epsilon_{t\bar{t}}^{SS}) \times \mathcal{L}} \quad (3)$$

where N is the observed/expected number of events, ϵ is the efficiency for any top quark pair events to enter our sample ($t\bar{t} \rightarrow$ inclusive in Table II), \mathcal{L} is the luminosity and $OS(SS)$ refers to opposite-sign(same-sign) samples.

The $t\bar{t}$ cross section in the individual dilepton channels is extracted by minimizing a negative log-likelihood function based on the Poisson probability of observing a number of events (N_j^{obs}) given the luminosity (\mathcal{L}_j), branching fraction (BR_j), efficiency (ϵ_j) and a number of background events (N_j^{bkg}): $-\log L(\sigma_j, \{N_j^{obs}, N_j^{bkg}, BR_j, \mathcal{L}_j, \epsilon_j\})$, while the combined cross section is measured by minimizing the sum of the negative log-likelihood functions for each individual channel (see [17] for more details on the method). The acceptances for opposite-sign and same-sign $t\bar{t}$ events are listed in Table II.

Systematic uncertainties are considered from the following sources: trigger, lepton ID, tau reconstruction, tau fake, jet energy calibration, primary vertex (PV) ID, b -tagging and MC normalization. The breakdown of uncertainties for the combined cross section is given in Table III. Systematic uncertainty on the primary vertex identification contains the uncertainties on PV selection and vertex z position simulation. Uncertainties on the MC normalization include normalization and flavor composition uncertainties. All uncertainties are treated as correlated between the $\mu\tau$ and $e\tau$ channels except for the individual muon or electron uncertainties and the background and MC statistics uncertainty.

We measure the top quark pair production cross section to be

$$\sigma(t\bar{t}) = 8.0_{-2.4}^{+2.8} (\text{stat})_{-1.7}^{+1.8} (\text{syst}) \pm 0.5 (\text{lumi}) \text{ pb} \quad (\mu\tau) \quad (4)$$

$$\sigma(t\bar{t}) = 8.6_{-2.6}^{+3.1} (\text{stat})_{-1.6}^{+1.6} (\text{syst}) \pm 0.5 (\text{lumi}) \text{ pb} \quad (e\tau) \quad (5)$$

$$\sigma(t\bar{t}) = 8.3_{-1.8}^{+2.0} (\text{stat})_{-1.2}^{+1.4} (\text{syst}) \pm 0.5 (\text{lumi}) \text{ pb} \quad (\text{combined}) \quad (6)$$

VI. CROSS SECTION \times BRANCHING RATIO EXTRACTION

For the measured cross section, many of the reconstructed tau candidates arise from jet or lepton fakes, as shown in Table I. The significant presence of $t\bar{t}$ events without real taus makes it advantageous to use them in measuring the $t\bar{t}$ cross-section.

TABLE III: Systematics for the measurement of $\sigma(t\bar{t})$.

	$\mu\tau$ $\Delta\sigma$	$e\tau$ $\Delta\sigma$	combined $\Delta\sigma$
Jet energy calibration	+0.30 -0.50	+0.33 -0.36	+0.43 -0.35
PV identification	+0.36 -0.34	+0.23 -0.37	+0.38 -0.21
Muon identification	+0.21 -0.20	-	+0.12 -0.12
Electron identification	-	+0.59 -0.53	+0.25 -0.24
Tau identification	+0.16 -0.15	+0.15 -0.15	+0.16 -0.16
Trigger	+0.00 -0.00	+0.12 -0.07	+0.14 -0.13
Fakes	+0.45 -0.42	+0.59 -0.53	+0.50 -0.49
b -tagging	+0.31 -0.34	+0.44 -0.41	+0.45 -0.37
MC normalization	+0.18 -0.18	+0.15 -0.15	+0.13 -0.13
Background/MC statistics	+1.46 -1.46	+1.19 -1.19	+1.00 -0.91
Other	+0.08 -0.08	+0.09 -0.10	+0.19 -0.18
Subtotal	+1.76 -1.67	+1.64 -1.59	+1.40 -1.24
Luminosity	± 0.49	± 0.52	± 0.51
Total	+1.83 -1.95	+1.72 -1.67	+1.49 -1.34

TABLE IV: Systematics for the measurement of $\sigma(t\bar{t}) \times \text{BR}(t\bar{t} \rightarrow \ell + \tau + 2b + 2\nu)$.

	$\mu\tau$ $\Delta\sigma \times \text{BR}$	$e\tau$ $\Delta\sigma \times \text{BR}$	combined $\Delta\sigma \times \text{BR}$
Jet energy calibration	+0.030 -0.023	+0.017 -0.019	+0.022 -0.020
PV identification	+0.020 -0.011	+0.019 -0.010	+0.019 -0.011
Muon identification	+0.004 -0.004	-	+0.005 -0.005
Electron identification	-	+0.027 -0.025	+0.015 -0.014
Tau identification	+0.006 -0.006	+0.006 -0.006	+0.007 -0.006
Trigger	+0.014 -0.013	+0.005 -0.003	+0.006 -0.006
Fakes	+0.034 -0.036	+0.030 -0.030	+0.032 -0.033
b -tagging	+0.025 -0.019	+0.022 -0.020	+0.023 -0.020
NLO $t\bar{t}$ cross-section	+0.027 -0.026	+0.023 -0.022	+0.025 -0.024
MC normalization	+0.009 -0.009	+0.006 -0.005	+0.007 -0.007
Background/MC statistics	+0.066 -0.066	+0.045 -0.045	+0.041 -0.037
Other	+0.004 -0.004	+0.007 -0.007	+0.010 -0.008
Subtotal	+0.093 -0.089	+0.074 -0.071	+0.072 -0.066
Luminosity	± 0.011	± 0.012	± 0.011
Total	+0.094 -0.090	+0.075 -0.072	+0.073 -0.067

In this section we measure the cross section times branching fraction $BR(t\bar{t} \rightarrow \ell + \tau + 2\nu + 2b)$ for dilepton events with a real muon or electron and a real tau decaying hadronically. Assuming a standard model $t\bar{t}$ cross section of 6.8 ± 0.6 pb [18, 19] and branching ratios for all other top decay modes, we include these contributions in the background estimate instead of considering them as signal. We use

$$\sigma_{t\bar{t}} \times BR(t\bar{t} \rightarrow \ell + \tau + 2\nu + 2b) = \frac{N_{\text{observed}} - N_{\text{expected background}}}{\epsilon \times \mathcal{L}}. \quad (7)$$

We consider the same set of systematic uncertainties as the cross-section measurement with the addition of theoretical uncertainty on the $t\bar{t}$ cross-section. The breakdown of uncertainties for the combined $\sigma \times \text{BR}$ is given in Table IV.

This results in

$$\sigma(t\bar{t}) \times BR(t\bar{t} \rightarrow \mu + \tau + 2\nu + 2b) = 0.18_{-0.11}^{+0.13} (\text{stat})_{-0.09}^{+0.09} (\text{syst}) \pm 0.01 (\text{lumi}) \text{ pb } (\mu\tau) \quad (8)$$

$$\sigma(t\bar{t}) \times BR(t\bar{t} \rightarrow e + \tau + 2\nu + 2b) = 0.19_{-0.10}^{+0.12} (\text{stat})_{-0.07}^{+0.07} (\text{syst}) \pm 0.01 (\text{lumi}) \text{ pb } (e\tau) \quad (9)$$

$$\sigma(t\bar{t}) \times BR(t\bar{t} \rightarrow \ell + \tau + 2\nu + 2b) = 0.19_{-0.08}^{+0.08} (\text{stat})_{-0.07}^{+0.07} (\text{syst}) \pm 0.01 (\text{lumi}) \text{ pb } (\text{combined}) \quad (10)$$

We determine a standard model expectation using the NLO cross section (6.8 pb) and branching ratios (Table V). The lepton can come directly from a W boson or from $W \rightarrow \tau\nu \rightarrow \ell\nu\nu\nu$ and the tau is only directly measured in the

TABLE V: Standard model branching ratios for top quark decays to appropriate muon, electron and tau final states. Values are taken from the 2006 PDG [20].

Observable final state	Branching ratio
$\text{BR}(t \rightarrow e\nu b) = \text{BR}(W \rightarrow e\nu_e) + \text{BR}(W \rightarrow \tau\nu_\tau \rightarrow e\nu_e\nu_\tau\nu_\tau)$	0.1276
$\text{BR}(t \rightarrow \mu\nu b) = \text{BR}(W \rightarrow \mu\nu_\mu) + \text{BR}(W \rightarrow \tau\nu_\tau \rightarrow \mu\nu_\mu\nu_\tau\nu_\tau)$	0.1252
$\text{BR}(t \rightarrow \tau_h\nu b) = \text{BR}(W \rightarrow \tau\nu_\tau) \times \text{BR}(\tau \rightarrow \text{hadrons} + \nu_\tau)$	0.0729

hadronic decay mode. Substituting these values into

$$\sigma \times \text{BR}(SM) = \sigma_{t\bar{t}} \times 2 \times \text{BR}(t \rightarrow \ell\nu b) \times \text{BR}(t \rightarrow \tau_h\nu b) \quad (11)$$

yields 0.12(0.13) pb in the $\mu\tau(e\tau)$ channel.

VII. CONCLUSIONS

We have performed the first DØ Run 2 top pair production cross section analysis dedicated to dilepton states including a hadronic tau decay. By selecting events with an isolated muon or electron, a hadronic tau, two or more jets (at least one of which is b -tagged) and missing transverse energy, we find a relatively large number of top candidates. We measure a top pair production cross section of $8.3^{+2.0}_{-1.8}$ (stat) $^{+1.4}_{-1.2}$ (syst) ± 0.5 (lumi) pb and a cross section times branching ratio of $0.19^{+0.08}_{-0.08}$ (stat) $^{+0.07}_{-0.07}$ (syst) ± 0.01 (lumi) pb in the $\mu\tau + e\tau$ combination. These are in good agreement with the standard model and limits on new physics contributions such as H^\pm are in progress.

Acknowledgments

We thank the staffs at Fermilab and collaborating institutions, and acknowledge support from the DOE and NSF (USA); CEA and CNRS/IN2P3 (France); FASI, Rosatom and RFBR (Russia); CAPES, CNPq, FAPERJ, FAPESP and FUNDUNESP (Brazil); DAE and DST (India); Colciencias (Colombia); CONACyT (Mexico); KRF (Korea); CONICET and UBACyT (Argentina); FOM (The Netherlands); PPARC (United Kingdom); MSMT (Czech Republic); CRC Program, CFI, NSERC and WestGrid Project (Canada); BMBF and DFG (Germany); SFI (Ireland); Research Corporation, Alexander von Humboldt Foundation, and the Marie Curie Program.

-
- [1] V.M. Abazov *et al.* [DØ Collaboration], “Measurement of $t\bar{t}$ Production Cross Section at $\sqrt{s} = 1.96$ TeV in Dilepton Final States Using 1 fb $^{-1}$ ”, DØ Note 5371-CONF, March, 2007. Available at <http://www-d0.fnal.gov/Run2Physics/WWW/results/prelim/TOP/T45>.
- [2] D. Acosta *et al.* [CDF Collaboration], “Measurement of $t\bar{t}$ Production Cross Section in $p\bar{p}$ Collisions at $\sqrt{s} = 1.96$ TeV using Dilepton Events, Phys. Rev. Lett. 93, 221802, 2004.
- [3] V.M. Abazov *et al.*, [DØ Collaboration], “Measurement of $t\bar{t}$ Cross Section in the Lepton+Jets Final State Using Lifetime Tagging on 900 pb $^{-1}$ ”, DØ Note 5355-CONF, March, 2007. Available at <http://www-d0.fnal.gov/Run2Physics/WWW/results/prelim/TOP/T43>.
- [4] A. Abulencia *et al.* [CDF Collaboration], “Measurement of $t\bar{t}$ Production Cross-Section in $p\bar{p}$ Collisions at $\sqrt{s} = 1.96$ TeV using Lepton+Jets Events with Jet Probability b -tagging”, Phys. Rev. D74, 072006, 2006.
- [5] V.M. Abazov *et al.* [DØ Collaboration], “Measurement of the $\sigma(p\bar{p} \rightarrow t\bar{t})$ Production Cross Section at $\sqrt{s} = 1.96$ TeV in the Fully Hadronic Decay Channel”, hep-ex/0612040, FERMILAB-PUB-06-426-E, submitted to Phys. Rev. D.
- [6] A. Abulencia *et al.* [CDF Collaboration], “Measurement of the $p\bar{p} \rightarrow t\bar{t}$ Production Cross Section in the All-Hadronic Decay Mode”, FERMILAB-PUB-07-316-E, 2007.
- [7] DØ Collaboration, “Measurement of $\sigma(p\bar{p} \rightarrow t\bar{t})$ in $\tau + \text{jets}$ channel”, DØ Note 5234-CONF, November, 2006. Available at <http://www-d0.fnal.gov/Run2Physics/WWW/results/prelim/TOP/T38>.
- [8] T. Andeen *et al.*, “The DØ Experiment’s Integrated Luminosity for Tevatron Run IIa”, FERMILAB-TM-2365-E (2006).
- [9] V.M. Abazov *et al.*, DØ Collaboration, “The Upgraded DØ Detector”, Nucl. Instrum. and Methods Phys. Res. A **565**, 463 (2006).
- [10] V.M. Abazov *et al.*, DØ Collaboration, “Measurement of the $t\bar{t}$ production cross-section in $p\bar{p}$ collisions using dilepton events”, FERMILAB-PUB-07-143E, 2007, submitted to Phys.Rev.D.

- [11] Jets are defined using the iterative seed-based cone algorithm with $\Delta R = \sqrt{(\Delta\phi)^2 + (\Delta y)^2} = 0.5$ (where ϕ is the azimuthal angle), including mid-points as described in Sec. 3.5 (p.47) of G. C. Blazey et al., in *Proceedings of the Workshop: "QCD and Weak Boson Physics in Run II"*, edited by U. Baur, R. K. Ellis, and D. Zeppenfeld, FERMILAB-PUB-00-297 (2000).
- [12] V.M. Abazov *et al.*, DØ Collaboration, "Measurement of $\sigma(p\bar{p} \rightarrow Z) \cdot \text{Br}(Z \rightarrow \tau\tau)$ at $\sqrt{s} = 1.96$ TeV", *Phys. Rev. D* **71**, 072004 (2004).
- [13] V.M. Abazov *et al.*, DØ Collaboration, "Evidence for production of single top quarks and first measurement of $|V_{tb}|$ ", *Phys. Rev. Lett.* **98**, 181802 (2007).
- [14] M.L. Mangano *et al.*, "ALPGEN, a generator for hard multiparton processes in hadronic collisions", *JHEP* **307**, 001 (2003), [arXiv:hep-ph/0206293].
- [15] T. Sjostrand, P. Eden, C. Friberg, L. Lonnblad, G. Miu, S. Mrenna and E. Norrbin, *Computer Phys. Commun.* **135**, 238 (2001).
- [16] R. Hamberg, W. L. van Neerven, and T. Matsuura, "A complete calculation of the order α_s^2 correction to the Drell-Yan K factor", *Nucl. Phys. B* **359**, 343 (1991), and errata in *B* **644**, 403 (2002).
- [17] DØ Collaboration, "Combined $t\bar{t}$ Production Cross Section at $\sqrt{s} = 1.96$ TeV in the Lepton+Jets and Dilepton Final States using Event Topology", DØ Note 4906, August, 2005.
- [18] M. Cacciari, S. Frixione, M.L. Mangano, P. Nason, and G. Ridolfi, *JHEP* **0404**, 068 (2004).
- [19] N. Kidonakis and R. Vogt, *Phys. Rev. D* **68**, 114014 (2003).
- [20] Yao, W.-M. *et al.*, "Review of Particle Physics", *J. Phys.*, **G33**, 1-1232 (2006).

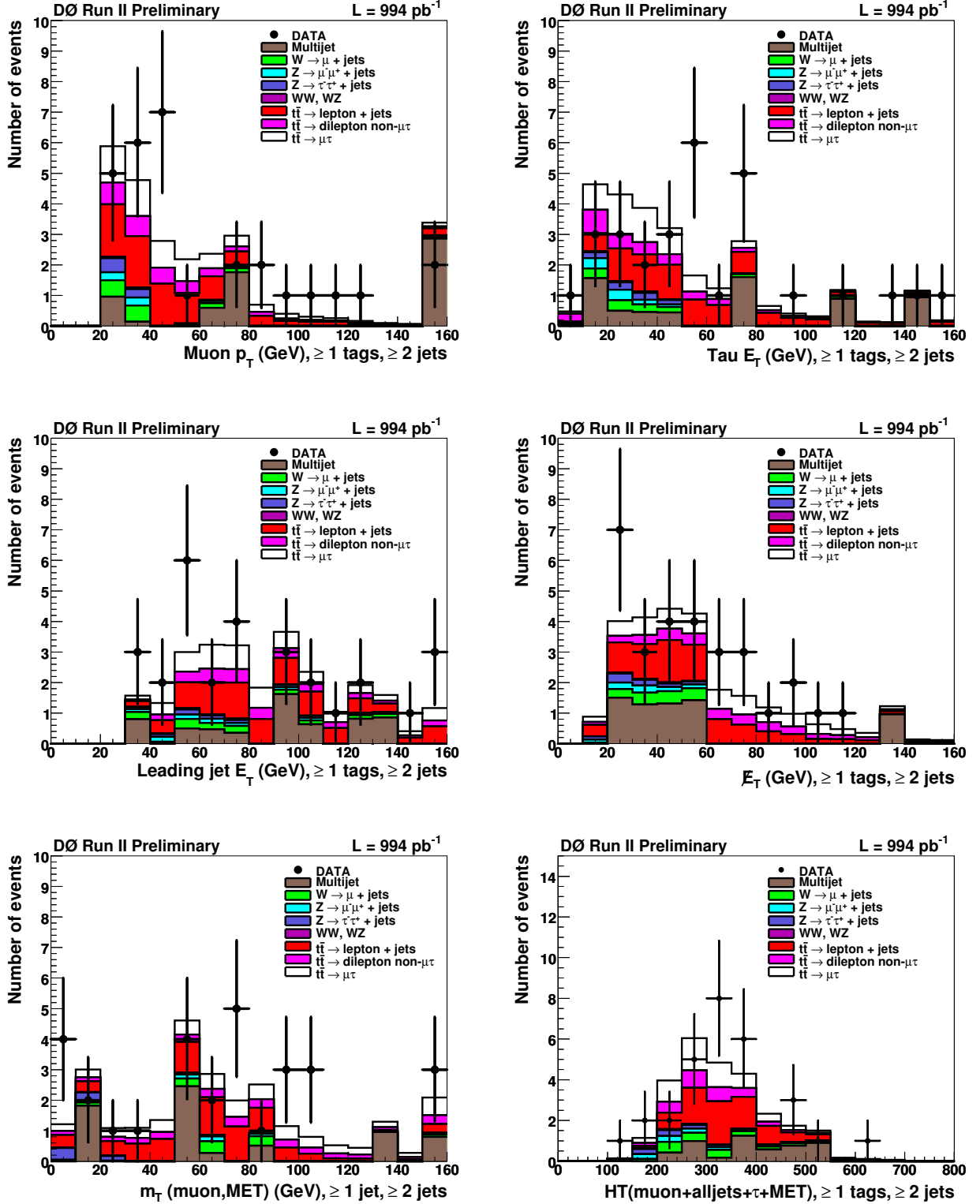


FIG. 6: Distributions comparing $\mu\tau$ data to expectations. This is done assuming a standard model cross section for top pair production. Overflows are placed in the rightmost bin. The distributions are: muon p_T (top left); τp_T (top right); leading jet p_T (middle left); missing transverse energy (E_T) (middle right); muon- E_T transverse mass, $m_T = \sqrt{(\cancel{E}_T + p_T^\mu)^2 - (\cancel{E}_x + p_x^\mu)^2 - (\cancel{E}_y + p_y^\mu)^2}$ (bottom left); H_T is the magnitude of the vector sum of the muon's, the tau's, all jets', and \cancel{E}_T 's transverse momentum (bottom right).

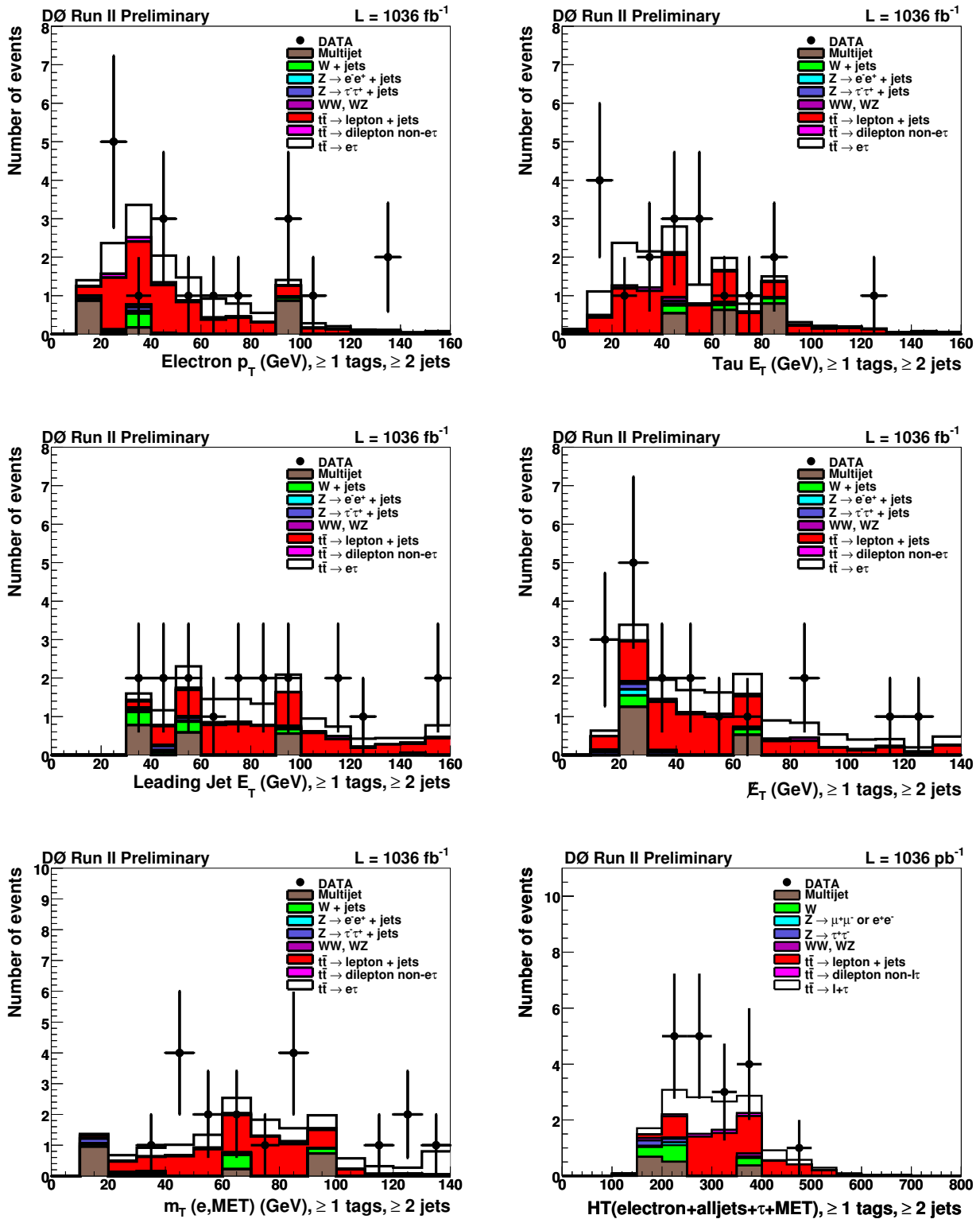


FIG. 7: Distributions comparing $e\tau$ data to expectations. This is done assuming a standard model cross section for top pair production. Overflows are placed in the rightmost bin. The distributions are: electron p_T (top left); τp_T (top right); leading jet p_T (middle left); missing transverse energy (E_T) (middle right); electron- E_T transverse mass, $m_T = \sqrt{(E_T + p_T^e)^2 - (E_x + p_x^e)^2 - (E_y + p_y^e)^2}$ (bottom left); H_T is the magnitude of the vector sum of the electron's, the tau's, all jets', and E_T 's transverse momentum (bottom right). In general the contribution from $t\bar{t} \rightarrow$ dilepton non- $e\tau$ sample can not be seen because it is smaller than the width of the histogram line.